AMERICAN SOCIETY FOR MICROBIOLOGY | Molecular and Cellular Biology®

RESEARCH ARTICLE

Vps34 and TOR Kinases Coordinate *HAC1* mRNA Translation in the Presence or Absence of Ire1-Dependent Splicing

Jagadeesh Kumar Uppala,[a] Sankhajit Bhattacharjee,[a] Madhusudan Dey[a]

[a]Department of Biological Sciences, University of Wisconsin—Milwaukee, Milwaukee, Wisconsin, USA

ABSTRACT In the budding yeast *Saccharomyces cerevisiae*, an mRNA, called *HAC1*, exists in a translationally repressed form in the cytoplasm. Under conditions of cellular stress, such as when unfolded proteins accumulate inside the endoplasmic reticulum (ER), an RNase Ire1 removes an intervening sequence (intron) from the *HAC1* mRNA by nonconventional cytosolic splicing. Removal of the intron results in translational derepression of *HAC1* mRNA and production of a transcription factor that activates expression of many enzymes and chaperones to increase the protein-folding capacity of the cell. Here, we show that Ire1-mediated RNA cleavage requires Watson-Crick base pairs in two RNA hairpins, which are located at the *HAC1* mRNA exon-intron junctions. Then, we show that the translational derepression of *HAC1* mRNA can occur independent of cytosolic splicing. These results are obtained from *HAC1* variants that translated an active Hac1 protein from the unspliced mRNA. Additionally, we show that the phosphatidylinositol-3-kinase Vps34 and the nutrient-sensing kinases TOR and GCN2 are key regulators of *HAC1* mRNA translation and consequently the ER stress responses. Collectively, our data suggest that the cytosolic splicing and the translational derepression of *HAC1* mRNA are coordinated by unique and parallel networks of signaling pathways.

KEYWORDS Hac1, Ire1, UPR, translation, Gcn2, Vps34, ER, TOR

An mRNA is translated into protein or stored for later translation in the cytoplasm. A large number of studies show that translationally repressed mRNAs are transiently stored into the RNA processing bodies (P-bodies) in many species (1, 2). Under favorable conditions, the translationally repressed mRNAs mobilize to access the translational machineries for fast and efficient protein synthesis (3), although it remains largely unknown how P-bodies store mRNAs and how mRNAs are translationally derepressed. In the budding yeast *Saccharomyces cerevisiae*, a number of untranslated mRNAs are reported to be associated with the P-body (4). For example, it has been shown that untranslated *HAC1* mRNA is associated with the P-body protein Lsm1 under glucose depletion condition, and under condition of cellular stress, *HAC1* mRNA migrates toward the endoplasmic reticulum (ER) (5). It has also been shown that *HAC1* mRNA contains an unusual intron in between two exons (Fig. 1) (6, 7). This intron is unusual because it is not spliced in the nucleus by the spliceosome but instead is retained in the mRNA that is exported to the cytoplasm. We and others have shown that the intron interacts with the 5′ untranslated region (5′-UTR) to form an RNA duplex (RD) near the mRNA cap (30 nucleotides away) (Fig. 1), which inhibits translation initiation under normal conditions (8, 9).

Under conditions of ER stress, such as when unfolded proteins accumulate inside the ER, a signaling pathway termed as the unfolded protein response (UPR) pathway is activated to alleviate the stress from yeast to humans (10). UPR in the yeast *S. cerevisiae* cells is initiated by an ER-resident endonuclease Ire1 that cleaves the intron at nucleotides G661 and G913 of *HAC1* mRNA (11–13). The cleaved mRNAs are then joined by

Citation Uppala JK, Bhattacharjee S, Dey M. 2021. Vps34 and TOR kinases coordinate *HAC1* mRNA translation in the presence or absence of Ire1-dependent splicing. Mol Cell Biol 41:e00662-20. https://doi.org/10.1128/MCB.00662-20.

Address correspondence to Madhusudan Dey, deym@uwm.edu.

Received 20 December 2020
Returned for modification 21 January 2021
Accepted 1 May 2021
Accepted manuscript posted online 10 May 2021
Published 23 June 2021

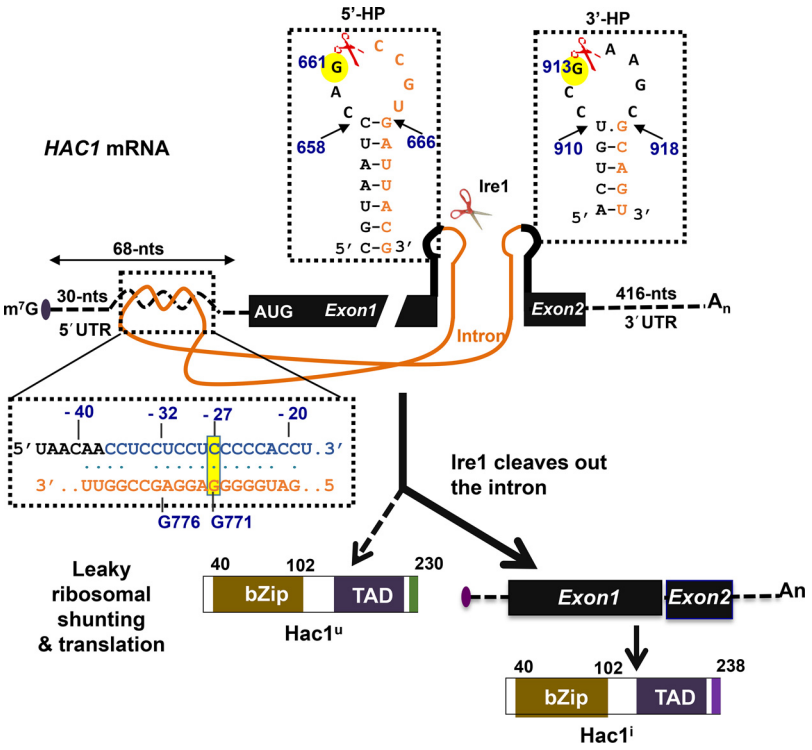

FIG 1 Translational fate of *HAC1* mRNA. The m^7G cap, 5′-UTR (68 nucleotides, [nts]) and 3′-UTR (416 nucleotides), two exons (black boxes, 661 and 56 nucleotides), intron, and polyadenylated tail (A_n) of *HAC1* mRNA are shown. The intron interacts with the 5′-UTR to form an RNA duplex (RD). Under ER stress conditions, Ire1 cleaves two phosphodiester bonds at the nucleotide positions G661 and G913 (shown by scissors). Both positions are present in the two RNA hairpins, referred to here as 5′-hairpin (5′-HP) and 3′-hairpin (3′-HP). The nucleotide compositions of the RD, 5′-HP, and 3′-HP are shown. The unspliced *HAC1* mRNA can translate an $Hac1^u$ protein (230 amino acids) by leaky scanning (16), which contains a bZIP domain, a transcription activation domain (TAD), and a short tail of 10 amino acids (green box). The spliced *HAC1* mRNA yields $Hac1^i$ protein (238 amino acids), containing a bZIP domain, a TAD, and an altered C-terminal tail of 18 amino acids (purple).

tRNA ligase Trl1 (14), resulting in a new codon in the open reading frame (ORF) at nucleotide G661 and a stop codon UAG at nucleotide 963. This spliced mRNA then translates a protein of 238 amino acids (referred to as $Hac1^i$; "i" indicates protein translated from the spliced mRNA) (Fig. 1). $Hac1^i$ is a transcription factor containing a basic leucine-zipper (bZIP) domain (residues 40 to 102) followed by a transcription activation domain that binds to the unfolded protein response element (UPRE) in the promoter of target genes and activates transcription of several chaperones and protein modifiers that enhance the protein folding capacity of cells (10).

In rare cases, ribosomes may bypass the 5′-UTR–intron RNA duplex in *HAC1* mRNA, resulting in leaky translation of a protein of 230 amino acids from the open reading frame (ORF) starting at the AUG codon of exon1 until the stop codon UGA at nucleotide 690 of the adjacent intron (15, 16). This translational product of *HAC1* mRNA is known as $Hac1^u$ protein (Fig. 1) ("u" indicates protein translated from the unspliced mRNA). Like $Hac1^i$, $Hac1^u$ is a transcription factor with a basic leucine zipper (bZIP) domain followed by a transcription activation domain (15). Both $Hac1^i$ and $Hac1^u$ isoforms share the same amino acid sequences until the position 220 (Fig. 1) but diverge beyond this position, with $Hac1^u$ having an additional 10 amino acids and $Hac1^i$ with an additional 18 amino acids. These 10 residues in the $Hac1^u$ isoform make it less stable (16); however, it can efficiently activate the UPR (15).

As described above, several studies suggest that translation of *HAC1* mRNA is repressed in the cytoplasm and derepressed after splicing; however, it is not clear how the splicing processes influence the translational derepression. To address these questions, we used

two *HAC1* variants that genetically separated the two primary biological processes involved in translational derepression and cytosolic splicing. Our studies suggest that the translational derepressionin *HAC1* mRNA is enhanced during ER stress with or without cytosolic splicing. Additionally, we show that the phosphatidylinositol 3-kinase (PI3-kinase) Vps34 and the nutrient-sensing kinases TOR (target of rapamycin) and Gcn2 (general control nonderepressible 2) were key translational regulators of *HAC1* mRNA. Collectively, our data suggest that the cytosolic splicing and the translational derepression of *HAC1* mRNA are coevolved and coordinated by unique and parallel networks of signaling pathways.

RESULTS

Genetic evidence of two RNA hairpins required for *HAC1* mRNA splicing *in vivo*. Under conditions of ER stress, Ire1 cleaves two phosphodiester bonds at nucleotides G661 and G913 in *HAC1* mRNA (11–13). *In silico* prediction and modeling of *HAC1* mRNA show that nucleotides G661 and G913 are located at two separate stem-loop RNA hairpins (referred here to 5′-HP and 3′-HP). Each of these RNA hairpins contains a loop of 7 nucleotides (5′-CAGCCGU-3′ or 5′-CCGAAGC-3′) and a stem of at least 5 bp (Fig. 1) (13, 17). The 5′-HP contains a canonical G-C base pair at the stem apex (i.e., between nucleotides C658 and G666), whereas the 3′-HP contains a noncanonical G-U base pair (i.e., between nucleotides U910 and G918). Thus far, no structural or genetic study has been done to provide evidence for the existence of these G-C and G-U base pairs. To provide the genetic evidence, here, we mutated these base pairing nucleotides and studied the sensitivity to Ire1-mediated splicing. The assumption behind the mutant design was that mutation will destroy the RNA hairpin structure, resulting in reduction or elimination of mRNA splicing. Thus, we created four single mutants (i.e., *HAC1*-C658G, *HAC1*-G666C, *HAC1*-U910G, and *HAC1*-G918U) and two double mutants (i.e., *HAC1*-C658G,G666C and *HAC1*-U910G,G918C). The single mutants were expected to destroy the base pair interaction in the RNA hairpin structure, and the double mutants were expected to restore the base pair interactions in opposite direction. These single and double mutants were introduced in the *hac1*Δ yeast strain. The resulting strains were then tested for their ability to grow on the tunicamycin medium and to splice *HAC1* mRNA under the condition of ER stress stimulated by dithiothreitol (DTT).

The wild type (WT), its isogenic *hac1*Δ and *hac1*Δ *ire1*Δ strains grew normally on the synthetic complete (SC) medium (Fig. 2A and C), showing that both *HAC1* and *IRE1* are nonessential genes. In contrast, both *hac1*Δ and *ire1*Δ strains, unlike the WT strain, grew on a medium containing an ER stressor tunicamycin only when complemented with a plasmid-borne *HAC1* and *IRE1* gene, respectively (Fig. 2A), suggesting a role of both Ire1 and Hac1 proteins in the tunicamycin-induced ER stress response. The reverse transcriptase PCR (RT-PCR) analysis showed a single population of *HAC1* mRNA in *ire1*Δ cells. In contrast, two distinct populations of *HAC1* mRNA were observed in WT cells grown in the presence of tunicamycin (Fig. 2B). These data are consistent with several reports that, under normal conditions, *HAC1* mRNA exists in a translationally repressed unspliced form (HAC1^{u}), whereas under ER stress condition, Ire1 cleaves *HAC1* mRNA to produce a spliced form (HAC1^{s}) (7, 8).

The *hac1*Δ strain containing a vector plasmid did not grow on the tunicamycin medium, nor did the same vector bearing the *HAC1*-C658G, *HAC1*-C666G, *HAC1*-U910G, or *HAC1*-G918U mutant (Fig. 2C and D, top) that was predicted to disrupt the RNA hairpin. The RT-PCR analysis showed only the unspliced form of *HAC1* mRNA (Hac1^{u}) in those single-mutant strains (Fig. 2C and D, bottom). These data suggested that each of those mutations eliminated *HAC1* mRNA splicing. In contrast, the *hac1*Δ strain containing an *HAC1*-C658G,G666C or *HAC1*-U910G,G918C double mutant was able to grow on the tunicamycin medium (Fig. 2C and D, top). Consistent with the tunicamycin-resistant phenotype, both unspliced (HAC1^{u}) and spliced (HAC1^{s}) forms of *HAC1* mRNA were observed (Fig. 2C and 2D, bottom). These data suggested that the base pair interaction at the stem apex was restored in the double mutant, thus facilitating mRNA splicing. We also mutated the nucleotide U910 to cytosine (C), generating a *HAC1*-U910C mutant, which

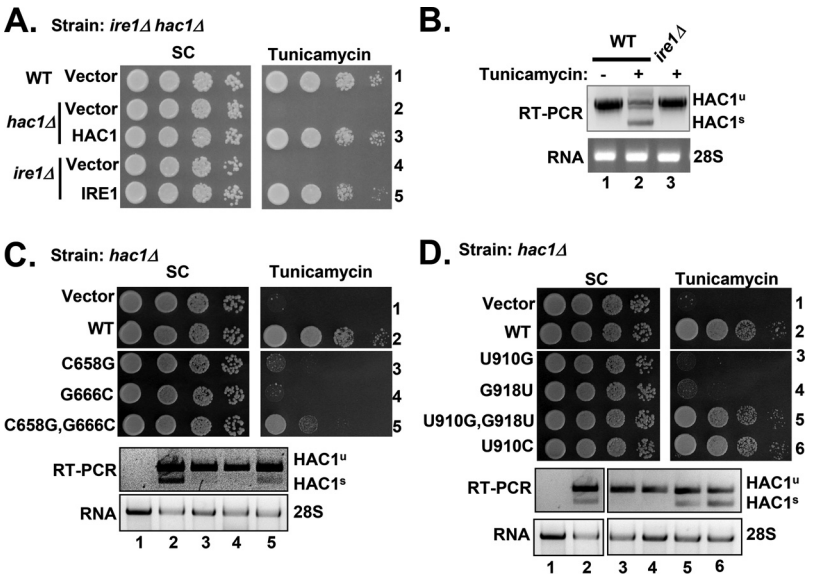

FIG 2 Ire1-mediated *HAC1* mRNA cleavage requires Watson-Crick base pairs in the cleavage RNA hairpins. (A) Growth of yeast cells on tunicamycin medium requires Ire1 and Hac1. WT and its isogenic *hac1*Δ or *ire1*Δ yeast strains containing a *URA3* plasmid (vector) or the same plasmid bearing an *HAC1* or *IRE1* gene were grown overnight, serially diluted, and spotted on the synthetic complete (SC) medium without uracil and the same medium containing tunicamycin. (B) ER stress activates *HAC1* mRNA splicing. Total RNA was extracted from the indicated yeast strains grown for 2 h in a liquid YEPD medium containing tunicamycin. RT-PCR was used to analyze the unspliced ($HAC1^u$) and spliced ($HAC1^s$) forms of *HAC1* mRNA. (C) Reciprocal exchange of nucleotides C658 and G666 restores *HAC1* mRNA splicing. (Top) An *hac1*Δ strain containing a URA3 plasmid (vector) or the same plasmid bearing the indicated *HAC1* mutant was tested for growth on the SC and tunicamycin media. (Bottom) RT-PCR was used to analyze the unspliced ($HAC1^u$) and spliced ($HAC1^s$) isoforms of *HAC1* mRNA in the above strains grown in the presence of tunicamycin. (D) Reciprocal exchange of nucleotides U910 and G918 restores *HAC1* mRNA splicing. An *hac1*Δ strain containing a URA3 plasmid (vector) or the same plasmid bearing the indicated *HAC1* mutant was tested for growth on the SC and tunicamycin media (top). RT-PCR was used to analyze the unspliced ($HAC1^u$) and spliced ($HAC1^s$) forms of *HAC1* mRNA in the above strains grown in the presence of tunicamycin (bottom).

was expected to form a canonical base pair interaction with G918 (Fig. 1). As expected, the *hac1*Δ strain containing the *HAC1*-U910C mutant was able to grow on the tunicamycin medium (Fig. 2D), and in those cells, efficient splicing of *HAC1* mRNA was observed (Fig. 2D, lane 6). Collectively, these data suggest that Ire1-catalyzed RNA cleavage requires Watson-Crick base pairs in two RNA hairpins, which are located at the *HAC1* mRNA exon-intron junctions.

Enhanced translation of *HAC1*-G771A,G661C mRNA under ER stress condition. Previously, Peter Walter's laboratory showed that a long-range base pair interaction between the 5′-UTR and intronic sequences inhibits translation of *HAC1* mRNA (8). We report that a single mutation of the nucleotide C(−27) at the 5′-UTR (relative to adenine [+1] of the AUG start codon) or its base-pairing partner nucleotide G771 at the intron is sufficient to derepress translational control of *HAC1* mRNA (Fig. 1) without the Ire1-mediated mRNA splicing (9). This splicing-independent translation of *HAC1* mRNA was evident from the observable traits that the *hac1*Δ strain containing a splice-defective *HAC1*-G661C mutant was sensitive to tunicamycin (Fig. 3A, row 2) but the same strain containing a *HAC1*-G661C,G771A mutant was resistant to tunicamycin (Fig. 3A, row 3). Consistent with the tunicamycin-resistant phenotype, the Hac1 protein was produced in cells containing the *HAC1*-G661C,G771A mutant under normal growth conditions (Fig. 3B, lane 3). The RT-PCR analysis showed that *hac1*Δ cells containing a WT *HAC1* allele expressed both unspliced and spliced forms of *HAC1* mRNA when grown in the presence of ER stressor DTT (Fig. 3C, lane 2). The same *hac1*Δ cells containing the *HAC1*-G661C,G771A or *HAC1*-G661C mutant expressed only the unspliced *HAC1* mRNA species (Fig. 3C, lanes 3 and 4), suggesting that the *HAC1*-G661C,G771A

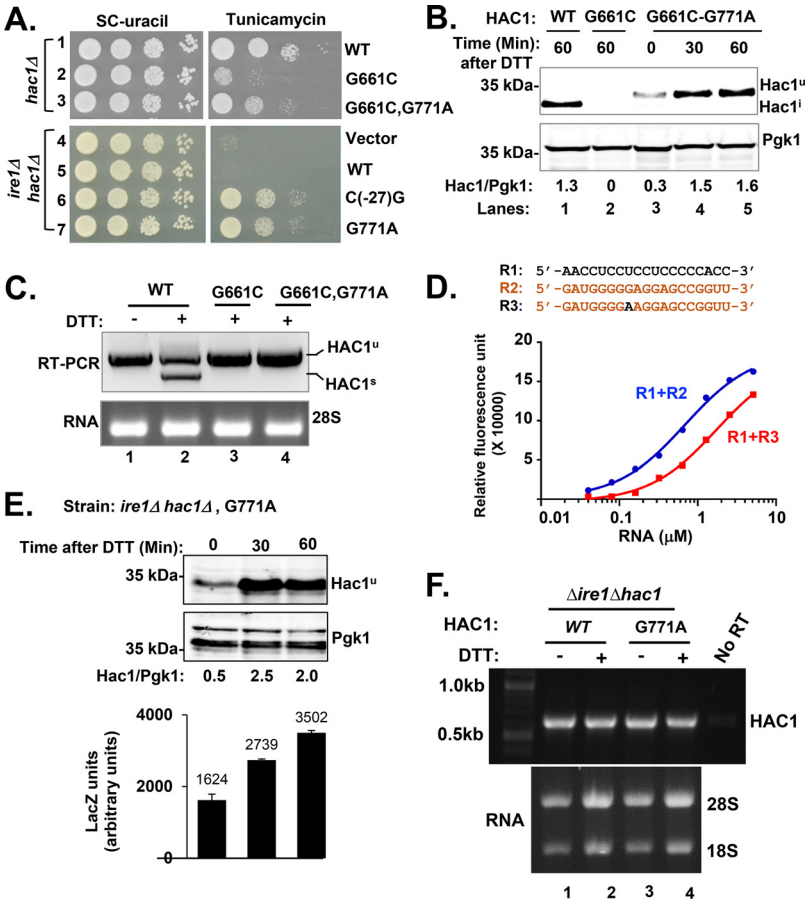

FIG 3 Translational derepression of *HAC1*-G771A and *HAC1*-G661C,G771A mRNA. (A) The *HAC1*-G661C,G771A mutant grows on the tunicamycin medium. The *hac1*Δ or *ire1*Δ *hac1*Δ strain containing the indicated *HAC1* mutants in a URA3 plasmid was tested for growth on the SC medium without uracil and the same medium containing tunicamycin. (B) Hac1^u expression from the *HAC1*-G661C, G771A mutant is enhanced under ER stress conditions. (Top) the *hac1*Δ strain containing the indicated *HAC1* mutants (WT, G661A, or G661A,G771A) were grown in the SC-uracil medium until OD_{600} reached ~0.6 to 0.8; 5 mM DTT was then added to cells. After indicated times (0, 30, and 60 min), cells were harvested, whole-cell extracts (WCEs) were prepared and subjected to Western blot analysis using anti-Hac1 and Pgk1 antibodies. The intensities of Hac1 and Pgk1 protein bands were measured by ImageJ software (bottom). The ratios of the Hac1 and Pgk1 protein band intensities are shown. Experiments were repeated twice. A representative result is shown. (C) The *HAC1*-G661C, G771A mutant is deficient in splicing. Total RNA was prepared from the *hac1*Δ strain containing the indicated *HAC1* mutants in a URA3 plasmid. RT-PCR was used to analyze the unspliced (HAC1^u) and spliced (HAC1^s) forms of *HAC1* mRNA. (D) *In vitro* reconstitution of the 5′-UTR and intron interaction. As indicated, three RNA oligonucleotides corresponding to the 5′-UTR (R1), the intron (R2), and the intron with a G771A mutation (R3) were synthesized from Sigma (USA). Mixtures of RNA oligonucleotides R1 and R2 and R1 and R3 were heated to 95°C for 5 min and then annealed at room temperature slowly. The RNA mixture was diluted, and SYBR green was added to the diluted samples. Samples were then read in a spectrophotometer. The relative fluorescence units were averaged and then plotted against the RNA concentrations. The calculated K_d values were 0.692 ± 0.18 for R1+R2 and 1.755 ± 0.02 for R1+R3. (E) Hac1^u expression from the *HAC1*-G771A mutant is enhanced during ER stress. WCEs were prepared from the *ire1*Δ *hac1*Δ strain containing the *HAC1*-G771A mutant and subjected to Western blot analysis using Hac1 and Pgk1 antibodies. The ratios of the Hac1 and Pgk1 protein band intensities are shown (top). The *ire1*Δ *hac1*Δ strain containing a *HAC1*-G771A allele in a *URA3* vector and an UPRE-driven LacZ reporter plasmid in a *LEU2* vector was grown as described in Fig. 3B. WCEs were prepared and subjected to β-galactosidase assay. The average values of three experiments are shown with standard errors (bottom). (F) ER stress does not induce the transcript levels of WT or *HAC1*-G771A mutant carried in plasmid. Total RNA was isolated from the *ire1*Δ *hac1*Δ strain containing WT HAC1 or *HAC1*-G771A mutant in a URA3 plasmid (bottom). Total RNA was reverse transcribed into cDNA. The synthesized cDNA was amplified by PCR using the exon1-specific primers of the *HAC1* gene (top). The RNA sample obtained from the WT cells was used as a PCR template without the reverse transcriptase reaction (no RT).

mutant produced the Hac1^u protein likely by an alternate cap-dependent translation initiation mechanism, such as leaky scanning (18) or ribosome jumping (19). Regardless of the underlying mechanism, our data suggest that unspliced *HAC1* mRNA can translate an active transcription factor and is capable of inducing the ER stress response.

To assess the impact of the G771A mutation on the 5′-UTR–intron RNA duplex, we performed an *in vitro* RNA duplex formation assay. Three RNA oligonucleotides (20 bases long) corresponding to the 5′-UTR and intronic sequences were synthesized as follows (Fig. 1): (i) RNA oligonucleotide 1 (R1), representing the 5′-UTR (5′-UAACCUCCUC CUCCCCCACC-3′); (ii) RNA oligonucleotide 2 (R2), representing the intron (5′-GAUGG GGGAGGAGCCGGUUG-3′); and (iii) RNA oligonucleotide 3 (R3), representing the intron-G771A mutation (5′-GAUGGGGAAGGAGCCGGUUG-3′; underlining indicates guanine was mutated to adenine) (Fig. 1 and 3D). The mixture of RNA oligonucleotides R1 and R2 or R1 and R3 was heated to 95°C for 5 min and then annealed at room temperature. The RNA mixture was diluted to obtain final concentrations ranging from 0.01 to 10 μM. An equal amount of SYBR green was added to each sample. The florescent intensity of each sample was then monitored. As shown in Fig. 3D, the fluorescence was detected in the mixture of R1 and R2 oligonucleotides at the concentration below 1 μM followed by a gradual increase in fluorescent intensities with the increase of RNA concentrations (the equilibrium-binding affinity, $K_d = 0.692\ \mu$M), suggesting that double-stranded RNA (dsRNA) was able to form complexes with SYBR green. The fluorescence was also detected in the mixture of R1 and R3 oligonucleotides, albeit at a slightly higher concentration of RNA ($K_d = 1.755\ \mu$M). The ~2.5-fold increase in the equilibrium-binding affinity from a fluorescence-based assay suggested that the single G771A mutation might cause a change in the local conformation but not the global conformation of the 5′-UTR–intron RNA duplex *in vitro*.

Next, we utilized both *HAC1*-G661C,G771A and *HAC1*-G771A mutants to assess the patterns of cooccurrence and mutual exclusivity between the cytosolic splicing and the translational derepression of *HAC1* mRNA under normal and ER stress conditions. The *hac1*Δ strain harboring an *HAC1*-G661C,G771A mutant was grown in synthetic complete (SC) medium in the presence of DTT (5 mM). Cells were harvested after 30 and 60 min. Whole-cell extracts were prepared and subjected to Western blot analysis. The Western blot showed that the Hac1 expression was induced at least 5-fold after 30 and 60 min of DTT treatment (Fig. 3B, compare lane 3 with lanes 4 and 5). These data suggest that ER stress induced the Hac1^u expression from the unspliced *HAC1*-G661C, G771A mRNA (i.e., Hac1^u isoform of 230 amino acids) and translational derepression can occur without splicing. Consistent with the earlier report (15), we also observed that the migration of Hac1^u protein produced from the *HAC1*-G661C,G771A mutant was slightly slower than the Hac1 protein produced from the WT *HAC1* mRNA after splicing (i.e., Hac1^i isoform of 238 amino acids) (Fig. 3B, compare lanes 1 and 3). A reasonable explanation is that the Hac1^u isoform likely undergoes altered posttranslational modifications, including phosphorylation. Nonetheless, these results provide evidence that translational derepression can occur without mRNA splicing.

To further confirm the above results, we investigated the effect of ER stress on Hac1^u expression from the *HAC1*-G771A and *HAC1*-C(−27)G mutants (Fig. 1) in the *ire1*Δ *hac1*Δ strain. As we reported earlier (9), the *ire1*Δ hac1Δ strain harboring the *HAC1*-G771A or *HAC1*-C(−27)G mutant was able to grow on the tunicamycin medium (Fig. 3A, rows 6 and 7). The growth was correlated with Hac1^u expression from the *HAC1*-G771A (Fig. 3E, lane 1) or *HAC1*-C(−27)G mutants (data not shown). Additionally, we observed a time-dependent increase in Hac1^u expression from the *HAC1*-G771A mutant when cells were grown in the presence of DTT (Fig. 3E). Consistently, we observed an increased expression of UPRE-driven LacZ reporter gene (Fig. 3E, bottom). From these results and the published report that the *HAC1* transcript level was increased ~2.5-fold during the ER stress (20), we interpreted that the enhanced Hac1^u expression from the *HAC1*-G771A mutant may be due to an activation of mRNA

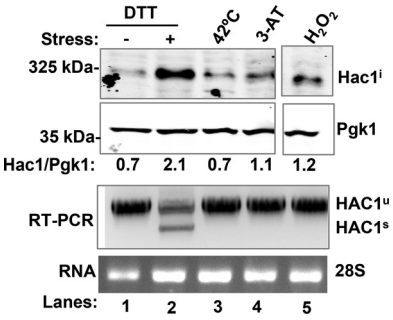

FIG 4 ER stress provokes Hac1^u expression from the *HAC1*-G771A mutant. The *ire1*Δ strain containing the *HAC1*-G771A mutant was grown in the SC-uracil medium in the presence of DTT (5 mM), 3-AT (30 mM), or H_2O_2 (0.5 mM) for 1 h. WCEs were prepared and subjected to Western blot analysis using anti-Hac1 and Pgk1 antibodies (top). The relative intensity of Hac1 protein band was measured by ImageJ software. The ratios of the Hac1 and Pgk1 protein band intensities are shown (bottom).

transcription leading to activation of translation and/or (2) specific activation of mRNA translation.

To test the above possibilities, we monitored the levels of WT and *HAC1*-G771A mRNAs during the ER stress. The *ire1*Δ *hac1*Δ strain containing a plasmid-borne WT HAC1 or *HAC1*-G771A mutant was grown in the presence of DTT for 1 h, and total RNA was isolated (Fig. 3F, bottom). Total RNA was reverse transcribed into cDNA. The synthesized cDNA was then amplified by PCR using the exon 1-specific primers of the *HAC1* gene (Fig. 3F, top). No significant difference in *HAC1* cDNA amplifications was observed when cells were grown in the presence of DTT (Fig. 3F). Also, no amplification of DNA was observed in the RNA sample directly taken as a template for PCR (Fig. 3F, No RT, lane 5), suggesting that DNA amplification was not from the contaminated genomic DNA. These results suggest that the enhanced Hac1^u expression from the *HAC1*-G771A mutant was due to an ER stress-induced activation of translational derepression. Together, we interpret that a single G771A mutation within the 5′-UTR–intron RNA duplex weakens the base pair interaction, thus facilitating helicases to melt the secondary structure or allowing ribosomes to bypass the secondary structure and decoding mRNA efficiently under conditions of ER stress.

Protein folding stress activates translation of the unspliced *HAC1*-G771A mRNA. To combat adverse cellular conditions, including high temperatures, hypoxia, and radiation, cells activate a rapid and transient gene expression program to adjust both RNA and protein synthesis. Thus, we investigated the Hac1^u expression from the *HAC1*-G771A mRNA in response to other cellular stresses, such as high temperature stress, H_2O_2-induced oxidative stress, and under condition of nutrient limitation. Compared to ER stress (DTT induction), a basal level of Hac1^u protein expression was observed when cells were grown at 42°C (Fig. 4, lane 3) or in the presence of H_2O_2 (Fig. 4, lane 5) and 3-AT (a nutrient stressor that inhibits histidine biosynthesis [21]) (Fig. 4, lane 4]. These data suggest that the oxidative and nutrient stresses have a minor effect on the production of Hac1^u protein production from the *HAC1*-G771A mRNA. We also observed that neither an oxidative nor nutrient stressor induced the *HAC1* mRNA splicing in wild-type cells (Fig. 4, bottom). Together, it appears that only the protein folding stress can activate translation from the unspliced *HAC1*-G771A mRNA.

Reduced *Hac1* expression from spliced mRNA in the Vps34 protein-null strain. Given that the ER stressor DTT or tunicamycin induces the Hac1^i expression, we hypothesized that any yeast deletion strain showing the tunicamycin-sensitive phenotype might produce a low level of Hac1^i protein. Therefore, we tested several kinase-deletion strains for their sensitivity to tunicamycin and their ability to produce Hac1^i protein. From those studies, we identified that the yeast strain lacking the PI3-kinase Vps34 (vacuolar protein sorting 34) was severely sensitive to tunicamycin (Fig. 5A, lane 4) and produced a reduced (~6-fold) amount of Hac1^i protein compared to its isogenic WT cells (Fig. 4B, compare lanes 2 and 4). An obligate partner of Vps34 is a pseudokinase, Vps15 (22). The

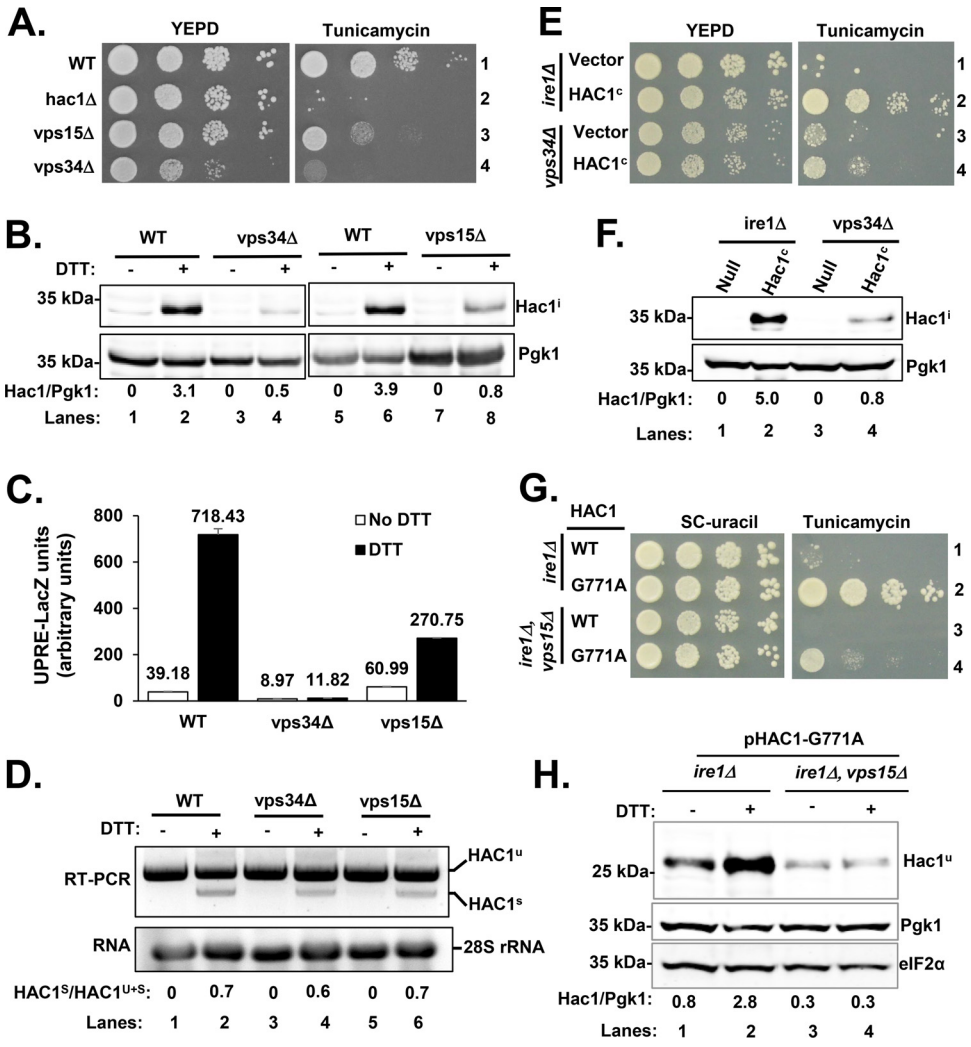

FIG 5 The PI3-kinase Vps34 contributes to Hac1^{i} expression. (A) The *vps34*Δ strain grows slowly on the tunicamycin medium. The indicated WT and its isogenic *hac1*Δ, *vps15*Δ, or *vps34*Δ yeast strains were tested for their growth on rich YEPD medium and the same medium containing tunicamycin. (B) Expression of Hac1^{i} protein is reduced in the *vps34*Δ strain. WCEs were prepared from the indicated yeast strain in the presence and absence of DTT and subjected to Western blot analysis using anti-Hac1 and Pgk1 antibodies. The intensities of Hac1 and Pgk1 protein bands were measured by ImageJ software, and the ratios of the Hac1 and Pgk1 bands are shown. (C) Reduced expression of UPRE-driven *LacZ* in both *vps34*Δ and *vps15*Δ strains. WCEs were prepared from the indicated yeast strains grown in the presence and absence of DTT and subjected to β-galactosidase assay. The average values of three experiments are shown with standard errors. (D) Deletion of Vps34 protein had no effect on *HAC1* mRNA splicing. Total RNA was prepared from the indicated WT, *vps34*Δ, and *vps15*Δ strains grown in a liquid YEPD medium containing tunicamycin. RT-PCR was used to analyze the unspliced (HAC1^{u}) and spliced (HAC1^{s}) forms of *HAC1* mRNA. (E) Reduced growth of the *vps34*Δ strain expressing an intronless *HAC1* variant. The indicated *ire1*Δ and *vps34*Δ strains containing a vector plasmid or the same vector plasmid harboring the intronless *HAC1* variant (HAC1^{c}) were tested for their growth on rich YEPD medium and the same medium containing tunicamycin. (F) Reduced expression of Hac1^{c} in the *vps34*Δ strain. WCEs were prepared from the indicated *ire1*Δ or *vps34*Δ strains expressing an Hac1^{c} derivative and subjected to Western blot analysis using Hac1 and Pgk1 antibodies. The intensities of Hac1 and Pgk1 protein bands were measured by ImageJ software, and the ratios of the Hac1^{c} and Pgk1 band intensities are shown. (G) The *ire1*Δ *vps15*Δ strain expressing *HAC1*-G771A allele grows slowly on the tunicamycin medium. The indicated *ire1*Δ strain and its isogenic *ire1*Δ *vps15*Δ strain expressing *HAC1*-G771A allele were tested for their growth on the medium containing tunicamycin. (H) Reduced expression of Hac1^{u} in the *ire1*Δ *vps15*Δ strain. WCEs were prepared from the strains shown in Fig. 4G and subjected to Western blot analysis using Hac1, Pgk1, and eIF2α antibodies.

*vps15*Δ strain exhibited a moderate tunicamycin-sensitive phenotype (Fig. 5A, lane 3) and produced a reduced (~4-fold) amount of Hac1^{i} protein compared to its isogenic WT cells (Fig. 5B, compare lanes 6 and 8). Consistently, the UPRE-driven LacZ reporter expressions were reduced ~10-fold in *vps34*Δ and ~3-fold in *vps15*Δ strains (Fig. 5C). However,

the spliced products (HAC1^s) of *HAC1* mRNA in *vps34*Δ and *vps15*Δ cells were very similar to its isogenic WT cells (Fig. 5D). These results suggest that kinases Vps34 and Vps15 regulate translational derepression of *HAC1* mRNA or are largely link to translational efficiency of the matured mRNA.

To further test if and how Vps34 contributed to translational efficiency of the matured *HAC1* mRNA, we introduced an intronless variant (Hac1^c) in the *vps34*Δ strain and monitored Hac1^i expression under normal growth condition. As expected, the *ire1*Δ strain constitutively expressed Hac1^i protein from the Hac1^c variant under a normal growth condition (Fig. 5E, lane 2). The Hac1^i expression from the Hac1^c variant was significantly reduced (~6-fold) in the *vps34*Δ strain compared to its isogenic *ire1*Δ strain (Fig. 5E, compare lanes 2 and 4), confirming that Vps34 plays an important role in translational control of *HAC1* mRNA.

To further confirm the role of Vps34 and Vps15 in ER stress response, we disrupted the *IRE1* gene in the *vps15*Δ and *vps34*Δ strains as described in Materials and Methods. Because the *ire1*Δ *vps34*Δ strain grew slowly, we used the *ire1*Δ *vps15*Δ strain for our studies. The *ire1*Δ *vps15*Δ strain containing the *HAC1*-G771A allele grew slowly compared to the *ire1*Δ strain containing the same *HAC1*-G771A allele (Fig. 5G, compare rows 4 with 2). The reduced growth was correlated with a reduced Hac1^u expression from the *HAC1*-G771A mRNA (Fig. 5H). Together, these findings confirm that Vps34 and Vps15 have a distinct stimulatory function in *HAC1* mRNA translation. Vps34 is the sole PI3-kinase in the budding yeast *S. cerevisiae* (22, 23), which is known to play critical roles in protein sorting (23) and autophagy (24). Our results discovered a new role for Vps34 in the ER stress response. Further research is needed to understand how Vps34 promotes Hac1 expression in response to ER stress. Indeed, these data suggest that the splicing and the translational derepression in *HAC1* mRNA occur together but are controlled by independent cellular processes.

Protein kinase Gcn2 activates *HAC1* mRNA translation. Two major signaling pathways, ISR (integrated stress response) (25) and TOR (target of rapamycin) (26), are known to control the rate of translation in many mRNAs. In mammalian cells, the ISR pathway is coordinated by a family of four kinases GCN2, PKR, PERK, and HRI. In yeast cells, only kinase Gcn2 signals the ISR. Each of these kinases are regulated by their unique regulatory domains, but phosphorylate a common substrate, initiation factor 2α (eIF2α (27). The phosphorylated eIF2α inhibits the function of guanine nucleotide exchange eIF2B, leading to translational activation of specific mRNAs, including Gcn4 in yeast cells (21) and ATF4 in mammalian cells (28). Gcn4 or ATF4 acts as the master transcription regulator for many enzymes that restructure metabolisms during starvation and stress responses. In *S. cerevisiae*, Patil and coworkers have shown that the transcription factor Gcn4 and its activator Gcn2 upregulate many UPR target genes (29).

To understand whether, and if so how, the ISR pathway regulates the *HAC1* translation, we examined the expression of the Hac1^u protein from *HAC1*-G771A or *HAC1*-G661C,G771A mutant in the *gcn2*Δ strain. Initially, we disrupted the chromosomal copy of the *IRE1* or *HAC1* gene from the *gcn2*Δ strain by a *KanMX4* cassette, creating the *ire1*Δ *gcn2*Δ and *hac1*Δ *gcn2*Δ strains, respectively. Then, we expressed the *HAC1*-G771A mutant in the *ire1*Δ *gcn2*Δ strain and the *HAC1*-G661C,G771A mutant in the *hac1*Δ *gcn2*Δ strain. The *ire1*Δ *gcn2*Δ strain containing the *HAC1*-G771A mutant (Fig. 6A, row 4) and the *hac1*Δ *gcn2*Δ strain containing the *HAC1*-G661C,G771A mutant (Fig. 6A, row 6) were able to grow on the tunicamycin medium. Interestingly, we observed that the Hac1^u expression from the *HAC1*-G661C,G771A mutant in *hac1*Δ *gcn2*Δ cells was ~50% lower than *hac1*Δ cells (Fig. 6B, Western blot, compare lanes 2 and 4). These results suggest that, under conditions of ER stress, the Gcn2 pathway is also activated, which contributes to translational derepression of *HAC1* mRNA by an unknown mechanism.

To further confirm the activation of the Gcn2 pathway under the condition of ER stress, we examined the phosphorylation status of its substrate eIF2α. A significant increase (~4-fold) in eIF2α phosphorylation was observed in cells when grown in the presence of the ER stressor DTT (Fig. 6C, compare lanes 1 and 4). The eIF2α

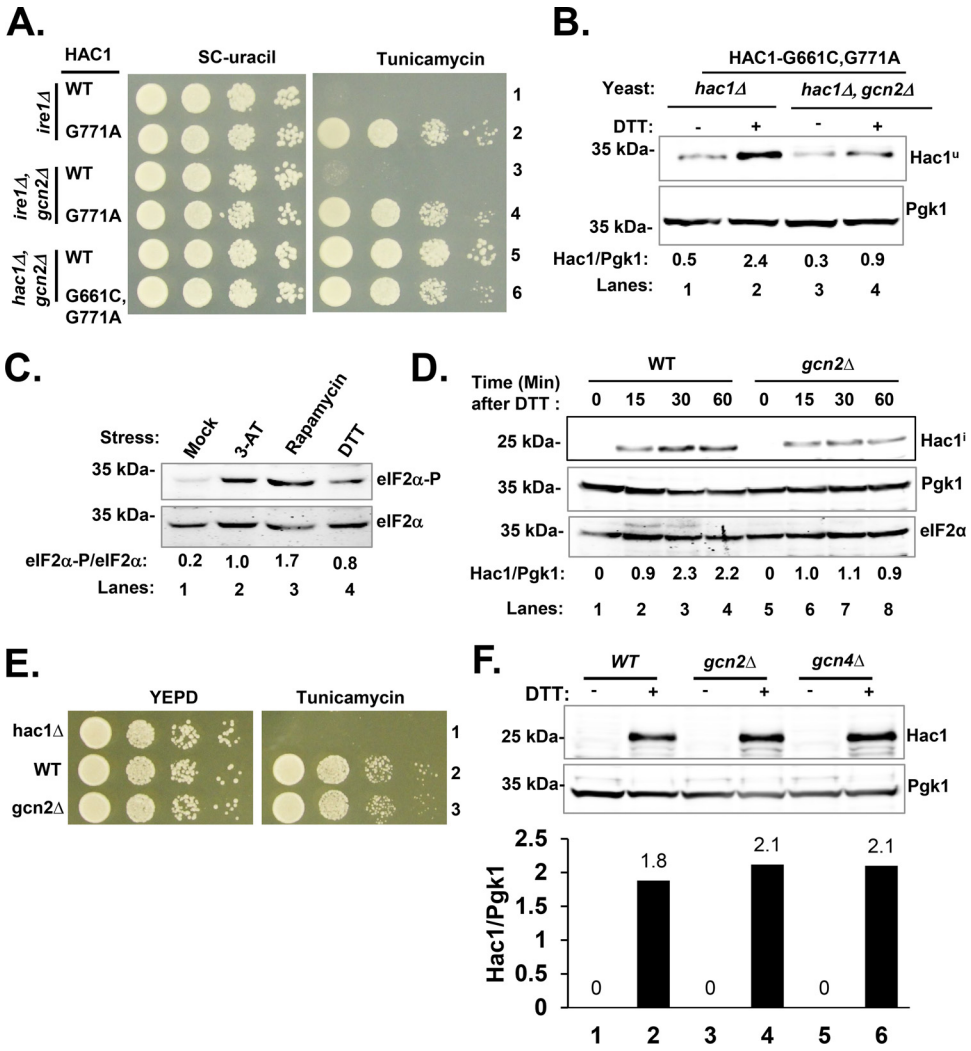

FIG 6 Translational activation of *HAC1*-G771A mRNA requires Gcn2 activation. (A) Analysis of yeast growth under ER stress condition. The *ire1*Δ, *ire1*Δ *gcn2*Δ, and *hac1*Δ *gcn2*Δ strains containing indicated WT *HAC1* and *HAC1*-G771A or *HAC1*-G661C,G771A mutant were tested for growth on SC and tunicamycin media. (B) Reduced expression of Hac1^u from *HAC1*-G771A mutant in the *gcn2*Δ strain. The *hac1*Δ or *hac1*Δ *gcn2*Δ strain containing the *HAC1*-G661C,G771A mutant was grown in the presence and absence of DTT. WCEs were prepared and subjected to Western blot analysis using Hac1 and Pgk1 antibodies. The ratios of the Hac1^u and Pgk1 band intensities are shown. (C) Increased phosphorylation of eIF2α upon DTT treatment. WT yeast cells were grown in the presence of 3-AT (30 mM), rapamycin (0.5 mM), or DTT (5 mM) for 1 h. WCEs were prepared and subjected to Western blot analysis using Ser-51 phospho-specific antibody against eIF2α (top). The membrane was stripped and reprobed with total eIF2α antibody (bottom). The ratios of the eIF2α-P and eIF2α band intensities are shown. (D) Modest reduction of Hac1^i expression in the *gcn2*Δ strain. WT and *gcn2*Δ strains were grown in the presence (+) and absence (−) of DTT. WCEs were prepared and subjected to Western blot analysis using Hac1, Pgk1, and eIF2α antibodies. The ratios of the Hac1 and Pgk1 protein band intensities are shown.

phosphorylation was also increased in cells grown in the presence of the histidine biosynthesis inhibitor 3-aminotriazol and the Tor kinase inhibitor rapamycin (30) (Fig. 6C, lanes 2 and 3). Together, these results are consistent with the earlier observation that the Gcn2 kinase function is important to upregulate many UPR target genes in the yeast *S. cerevisiae* (29). Consistently, we observed that Hac1^i expression from the spliced mRNA was reduced ~50% in cells lacking the Gcn2 kinase when treated with DTT for 30 or 60 min (Fig. 6D, Western blot, Hac1, compare lanes 3, 4, 7, and 8). However, both *gcn4*Δ and *gcn2*Δ strains grew on the tunicamycin medium (Fig. 6E) and produced Hac1^i protein like WT cells when grown in the presence of an ER stressor DTT (Fig. 6F, compare lanes 2, 4, and 6). Therefore, it is not yet clear how Gcn4

combines with Hac1 and activates transcription of UPR target genes. Nonetheless, our observations suggest that not only Gcn2 but also other signaling pathways are likely to be involved in promoting the translational derepression of *HAC1* mRNA.

Tor1 and Tor2 kinases contribute to Hac1 protein expression. The TOR pathway is coordinated by two distinct signaling complexes, TOR complex 1 (TORC1) and TOR complex 2 (TORC2) (26). The sole TOR kinase in mammalian cells (mTOR) forms both TORC1 and TORC2, whereas two distinct TOR kinases (Tor1 and Tor2) in the budding and fission yeasts form two respective TOR complexes. The best-characterized downstream targets of TOR complexes are S6 kinases (S6Ks) (31) and eIF4E-binding proteins (4E-BPs) in mammalian cells (32), whereas Sch9 kinase (33) and Eap1 in yeast cells (34). S6Ks regulate the functions of the helicase eIF4A, which unwinds the mRNA secondary structure during translation (35). The 4E-BPs, conversely, regulate the binding of eIF4E to the mRNA cap (36).

To determine if the TOR pathway regulates the *HAC1* translation, we examined the Hac1 expression in a *tor1*Δ strain harboring a temperature-sensitive allele of *tor2* (i.e., *tor1*Δ *tor2*^{ts} strain, gift from N. Hall). As reported earlier (37), the *tor1*Δ *tor2*^{ts} strain was able to grow at 37°C only when complemented by a plasmid-borne WT Tor2 but not by an inactive Tor2-D2298E mutant (Fig. 7A). We disrupted the chromosomal copy of the *IRE1* gene in the *tor1*Δ *tor2*^{ts} strain and its isogenic WT strain (JK9-3da) by a *KanMX4* cassette, creating the *ire1*Δ and *ire1*Δ *tor1*Δ *tor2*^{ts} strains, respectively. As expected, the *ire1*Δ strain (isogenic of JK9-3da) expressing the *HAC1*-G771A mutant grew on the tunicamycin medium at both 25°C and 37°C (Fig. 7B, rows 2 and 4), and the *ire1*Δ *tor1*Δ *tor2*^{ts} strains expressing the *HAC1*-G771A mutant grew on the tunicamycin medium only at 25°C (Fig. 7B, row 4). Interestingly, we observed that the Hac1^{u} expression from the *HAC1*-G771A mutant was reduced ~50% in the *ire1*Δ *tor1*Δ *tor2*^{ts} cells compared to its isogenic *ire1*Δ cells when grown at 37°C in the presence of DTT for 2 or 4 h (Fig. 7C, compare lane 2 with 4 and lane 6 with 8). These data suggest that Tor kinases play a significant role in translational derepression of *HAC1* mRNA.

To confirm our results, we examined the expression of Hac1^{i} protein from the spliced mRNA in the *tor1*Δ *tor2*^{ts} strain grown in the presence of DTT at a nonpermissive temperature (37°C). Interestingly, we observed that Hac1^{i} expression under an ER stress condition was reduced almost 50% in the *tor1*Δ *tor2*^{ts} strain compared to its isogenic WT strain (Fig. 7D, Hac1, compare lanes 3 and 5). Additionally, we observed that *UPRE*-driven LacZ expression was reduced (~2-fold) in the *tor1*Δ *tor2*^{ts} *strain* when grown at 37°C (Fig. 7E). These data confirm that the TOR pathway along with the Gcn2 pathway synergistically upregulates the *HAC1* mRNA translational derepression. Together, these data suggest that both ISR and TOR pathways coordinate the *HAC1* mRNA translation during the ER stress response.

DISCUSSION

In this report, we provide molecular genetic evidence that Ire1-mediated RNA cleavage requires Watson-Crick base pairs in two RNA hairpins (Fig. 2). Then, we provide evidence that the regulation of translational derepression of *HAC1* mRNA is independent of its cytoplasmic splicing, utilizing a *HAC1*-G771A mRNA variant that can translate Hac1^{u} protein from the unspliced mRNA under normal conditions. The same *HAC1*-G771A mRNA can also translate Hac1^{i} protein from the spliced mRNA during ER stress. Here, we show that the Hac1^{u} protein expression from the unspliced *HAC1*-G771A mRNA is enhanced during ER stress (Fig. 3 and 4). In parallel, we show that the PI3 kinase Vps34 does not play a major role in the cytosolic splicing of *HAC1* mRNA but significantly contributes to translation from the spliced *HAC1* mRNA (Fig. 5). These findings further highlight the fact that the cytoplasmic splicing and the translation of *HAC1* mRNA are regulated independently. Additionally, we show that the Gcn2 and TOR kinase functions are important to upregulate the translational derepression of *HAC1* mRNA in response to cellular stress (Fig. 6 and 7).

Under conditions of ER stress, *HAC1* (5) mRNA in yeast cells or its counterpart *XBP1* (38) mRNA in human cells colocalizes with the RNase Ire1 that is concomitantly

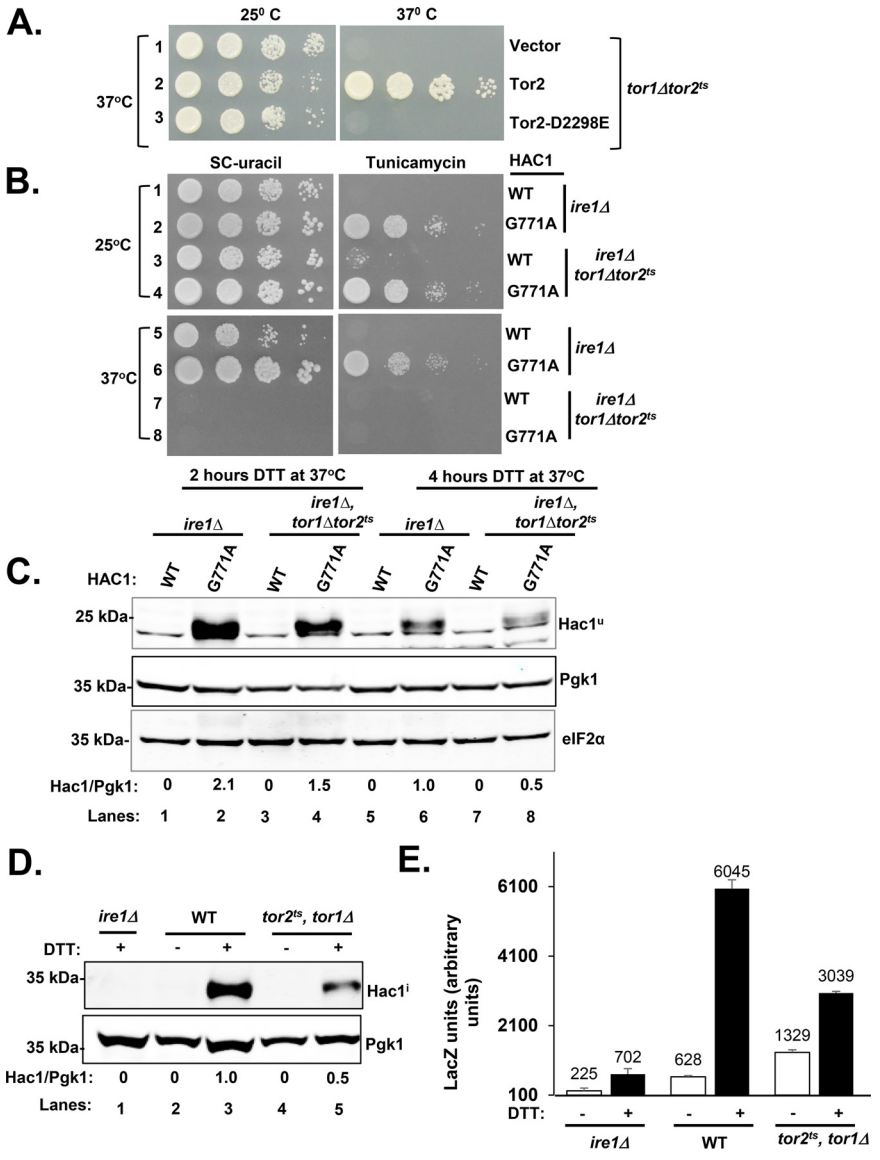

FIG 7 Translational activations of *HAC1* mRNA requires TOR kinase function. (A) The *tor1*Δ *tor2*^{ts} strain does not grow at 37°C. The *tor1*Δ *tor2*^{ts} strains expressing WT Tor2 and Tor2-D2298E mutant were tested for growth at 25°C and 37°C. (B) The *ire1*Δ *tor1*Δ *tor2*^{ts} strain containing the *HAC1*-G771A mutant grows under the ER stress condition. The indicated *ire1*Δ or *ire1*Δ *tor1*Δ *tor2*^{ts} strain containing WT *HAC1* or *HAC1*-G771A mutant was tested for growth on SC and tunicamycin media at 25°C and 37°C. (C) Reduced expression of Hac1^{u} from the *HAC1*-G771A mutant in the *ire1*Δ *tor1*Δ *tor2*^{ts} strain. The indicated yeast strains were grown in the presence of DTT at 37°C for 2 or 4 h. WCEs were prepared and subjected to Western blot analysis using Hac1^{u}, Pgk1, and eIF2α antibodies. The ratios of the Hac1^{u} and Pgk1 protein band intensities are shown. (D) Reduced expression of Hac1^{i} in the *tor1*Δ *tor2*^{ts} strain. The indicated yeast strains were grown in the presence (+) and absence (−) of DTT. WCEs were prepared and subjected to Western blot analysis using Hac1 and Pgk1 antibodies. The ratios of the Hac1^{i} and Pgk1 protein band intensities are shown. (E) Reduced expression of UPRE-driven *LacZ* in the *tor1*Δ *tor2*^{ts} strain. WCEs were prepared from the indicated yeast strains grown at 37°C for 4 h in the presence (+) and absence (−) of 5 mM DTT and subjected to β-galactosidase assay. The average values of three experiments are shown with standard errors.

activated by dimerization, oligomerization, and autophosphorylation (39, 40). Active Ire1 then cleaves two RNA hairpins in *HAC1* (Fig. 1) or *XBP1* mRNA, thus removing the intron. Removal of a part of the mRNA sequence, in either case, results in a shift in the open reading frame and the production of an active transcription factor. Here, we provide the molecular genetic evidence that Ire1 cleavage at sites G661 and G913 require the Watson-Crick base pair interaction in two RNA hairpins (Fig. 2), and a single

mutation in either site of the splicing hairpin (e.g., C658 at the 5′-HP or U910 at the 3′-HP) (Fig. 1) can reduce the overall splicing events. Recently, Cherry et al. have shown by Northern blotting analysis that *HAC1* mRNA is predominantly and promiscuously spliced under normal condition in yeast cells lacking the 3′→5′ exonuclease Xrn1 (41). However, we observed that the *xrn1*Δ strain produced Hac1 protein only under conditions of ER stress (data not shown). Thus, the proposed *HAC1* mRNA intermediates observed by Cherry et al. may not be the precise translationally active splicing products, and the question remains as to what extent Xrn1 contributes to the UPR.

Yeast tRNA ligase Trl1 (14) has been reported to ligate two cleaved *HAC1* exons to produce a matured mRNA that yields Hac1^{i} protein. Crystal structures of Ire1 (39, 40) and Trl1 (42) and the relevant functional studies suggest that the Ire1-Trl1-mediated *HAC1* mRNA splicing occurs in stepwise processes. First, multiple Ire1 molecules cluster across the ER membrane to form an oligomer of dimers, with each dimer containing twin RNase catalytic centers (40). Second, only one RNA hairpin is oriented in each dimeric RNase catalytic center; that means 5′-HP and 3′-HP are oriented in two separate RNase catalytic centers. Finally, the exon-exon ligation takes place by conformational changes and zipping of two RNA hairpins (43). While it is still unclear how 5′-HP and 3′-HP juxtapose within the RNase catalytic center, the exact mechanism of Ire1-Trl1-mediated *HAC1* mRNA splicing awaits a cocrystal structure of Ire1 or Trl1 bound to 5′-HP or 3′-HP. Previously, Mori et al. reported that a Trl1 or Rlg1 ortholog from *Arabidopsis thaliana* could ligate *HAC1* exons, but the spliced mRNA was unable to activate the UPR (44). They suggested that splicing was not sufficient to restore the UPR. Similarly, we observed that the spliced *HAC1* mRNA was unable to fully restore UPR in the *vps34*Δ strain (Fig. 5). Thus, it appears that while both splicing and translational derepression of *HAC1* mRNA can occur independently during ER stress, an optimum UPR activation requires coordination of both processes.

Cells have evolved multiple strategies to regulate protein synthesis in response to changing environments, such as nutrient deprivation, genotoxic stress, and viral infection. Translational regulation may be globally mediated by general translation factors or transcript specifically mediated by its own 5′-leader and/or 3′-trailer sequences. These UTRs vary in their lengths, ranging from a few nucleotides to several thousand nucleotides (45). The average length of 5′-UTRs is ~100 bases in yeast (46) and ~800 bases in human (47). They may fold into a specific structure, ranging from a simple hairpin to a more complex three-dimensional structure. These structures include ribozyme, iron-responsive elements, internal ribosomal entry sites (IRES), and riboswitches. UTRs may contain *cis* regulatory motifs, including upstream AUG, microRNA recognition motif (48, 49), and Kozak sequence (50). These *cis* motifs may control translational output, residing inside/outside of the secondary structure with or without their cognate *trans*-acting factors (51, 52). Several self-folded structures within *HAC1* mRNA control its splicing and translation (Fig. 1). These structures include a cap-proximal RNA duplex (RD) formed by 5′-UTR and intron (8, 9), two splicing RNA hairpins (13), and a 3′-bipartite element present within its 3′-UTR (5) (Fig. 1). We have shown previously that the 5′-UTR–intron RNA duplex inhibits initiation of translation; however, it remains poorly understood how *HAC1* splicing exerts an effect on the translational derepression.

Our results show that the Hac1^{u} protein is expressed from the *HAC1*-G771A mRNA under normal conditions, likely providing an example of alternate noncanonical cap-dependent translation initiation mechanism. Several cap-dependent alternate mechanisms of translation initiation have been reported in mammalian cells. These include eIF3d-dependent (53) and RNA-helicase DDX3-dependent initiation mechanisms (54). Additionally, Guan et al. reported that the eIF3 complex has a specialized role in reprograming translation initiation during chronic stress (55). At this point, it is not clear how *HAC1*-G771A mRNA uses a cap-dependent mechanism because a proximal secondary structure (Fig. 1) likely impedes ribosome or helicase recruitment. A typical 40S ribosomal subunit is known to occupy at least 20 nucleotides (nt) upstream and 11 nt downstream of the AUG start codon (56). It has also been shown that ~30 nt of 5′-UTR is needed for efficient

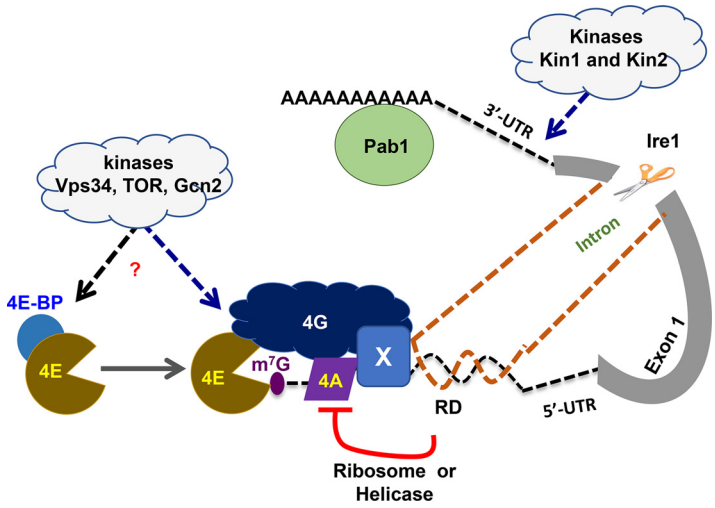

FIG 8 Proposed model for translational derepression of *HAC1* mRNA. The color scheme of *HAC1* mRNA is the same as in Fig. 1. The intron interacts with the 5′-UTR to form an RNA duplex (RD), thus inhibiting ribosome or helicase recruitment. The diagram shows the core components of the (m^7G) cap complex (eIF4E, eIF4G, and eIF4A) with its RD bound to a suppressor protein (blue box). The diagram also shows the proposed assembly of eIF4G, eIF4E, and eIF4A on the (m^7G) cap and their regulation by kinases Vps34, TOR, and Gcn2 as well as the proposed role of Kin kinases (65) in splicing of *HAC1* mRNA.

recognition of the AUG (57) codon with a purine at the position −3 and a guanine at the position +4 (58). Consistently, the recent translation complex profiling sequencing (TCP-seq) data reveal that the 40S ribosome-protected fragments at the 5′-UTR ranges from 19 nt to 75 nt (59). Thus, it appears that m^7G-cap along with its adjacent 30 nt are likely required for efficient recruitment of 43S-PIC. Based on this information, we posit that *HAC1* mRNA remains transnationally silent likely because 43S-PIC is unable to assemble on 5′-UTR (Fig. 3A). Thus, it is reasonable to think that a translational suppressor protein (Fig. 8) is likely bound to 5′-UTR–intron RNA duplex and keeps the *HAC1* mRNA translationally repressed. The G771A mutation weakens the binding of the suppressor protein to the RNA duplex, resulting in partial release of translation. Indeed, further studies are needed to understand the molecular details of how the ER stress activates translation from *HAC1* mRNA.

In an effort to understand how an ER stress stimulates other signaling pathways, we monitored the Hac1 expression in yeast strains lacking the kinase Gcn2, TOR, or Vps34 (Fig. 5 to 7). In the *gcn2*Δ strain, we found a modest reduction of Hac1 protein. Additionally, we observed that eIF2α phosphorylation was elevated when yeast cells were grown under a condition of ER stress (Fig. 6). This result is in line with the previous studies in mammalian cells that eIF2α phosphorylation was increased in *PERK*$^{-/-}$ but not in tunicamycin-treated PERK$^{-/-}$ *GCN2*$^{-/-}$ fibroblasts (60). Together, it appears that the ER stress response is associated with the activation of GCN2 kinase. Like *gcn2*Δ cells, the *tor1*Δ *tor2*^{ts} cells produced a low level of Hac1 protein (Fig. 7), suggesting that Tor1 and Tor2 kinases play an important role in the ER stress response. The Tor kinase function in yeast cells seems to be channeled through two major substrates: the kinase Sch9 (an ortholog of human S6K) (33) and the PP2A phosphatase subunit Tap42 (ortholog of human α4) (61, 62). However, we did not find any significant difference in Hac1 expression in a yeast strain lacking the kinase Sch9 (data not shown). Therefore, it is possible that, during the ER stress, TOR kinases evoke a unique signaling route, which is mediated by unknown intermediaries. Similar to *gcn2*Δ and *tor1*Δ *tor2*^{ts} strains, both *vps15*Δ and *vps34*Δ strains expressed a low level of Hac1 protein under condition of ER stress (Fig. 5). Collectively, these results uncover a new role

TABLE 1 List of yeast strains used in this study

Yeast strain	Genotype	Reference or study
WT (By4771)	*MAT***a** *his3-Δ1 leu2-Δ0 met5-Δ0 ura3-Δ0*	Deletion collection
*ire1*Δ strain	*MAT***a** *his3-Δ1 leu2-Δ0 met5-Δ0 ura3-Δ0 ire1::kanMX*	Deletion collection
*ire1*Δ*-hphMX* strain	*MAT***a** *his3-Δ1 leu2-Δ0 met5-Δ0 ura3-Δ0 ire1::hphMX*	This study
*hac1*Δ strain	*MAT***a** *his3-Δ1 leu2-Δ0 met5-Δ0 ura3-Δ0 hac1::kanMX*	Deletion collection
*hac1*Δ*-hphMX* strain	*MAT***a** *his3-Δ1 leu2-Δ0 met5-Δ0 ura3-Δ0 hac1::hphMX*	This study
*ire1*Δ *hac1*Δ strain	*MAT***a** *his3-Δ1 leu2-Δ0 met5-Δ0 ura3-Δ0 hac1::kanMX ire1::NatMX*	Lee et al. (39)
*vps15*Δ strain	*MAT***a** *his3-Δ1 leu2-Δ0 met5-Δ0 ura3-Δ0 vps15::kanMX*	Deletion collection
*vps34*Δ strain	*MAT***a** *his3-Δ1 leu2-Δ0 met5-Δ0 ura3-Δ0 Vps34::kanMX*	Deletion collection
*ire1*Δ *vps15*Δ strain	*MAT***a** *his3-Δ1 leu2-Δ0 met5-Δ0 ura3-Δ0 vps15::kanMX ire1::hphMX*	This study
*gcn2*Δ strain	*MAT***a** *his3-Δ1 leu2-Δ0 met5-Δ0 ura3-Δ0 gcn2::kanMX*	Deletion collection
*gcn2*Δ *hac1*Δ strain	*MAT***a** *his3-Δ1 leu2-Δ0 met5-Δ0 ura3-Δ0 gcn2::kanMX hac1::hphMX*	This study
WT (JK9-3da)	JK9-3da *ade2 his3 HIS4*	Gift from Michael N. Hall (66)
*tor1*Δ *tor2*^{ts} strain	JK9-3da *ade2 his3 HIS4 tor1::HIS3 tor2::ADE2-3/YCplac111::tor2-21*^{ts}	Gift from Michael N. Hall (66)
*ire1*Δ *tor1*Δ *tor2*^{ts} strain	JK9-3da *ade2 his3 HIS4 tor1::HIS3 tor2::ADE2-3/YCplac111::tor2-21*^{ts} *ire1::hphMX*	This study

of Vps34 in the ER stress response, apart from its known functions in autophagic, phagocytotic, and nutrient-sensing pathways (22–24).

In summary, results from this study provide clear evidence that splicing and translational derepression can occur simultaneously and independently. Here, we propose a model for translational derepression of *HAC1* mRNA. The cap-proximal 5′-UTR–intron RNA duplex (30 nucleotide away from the cap) (Fig. 1) in *HAC1* mRNA likely combine with the cap complex and a putative suppressor to form an inhibitory complex that precludes weaker recruitment of ribosomes or helicase eIF4A (Fig. 8). The weaker recruitment of ribosome or helicase results in less unwinding of the secondary structure, thus keeping *HAC1* mRNA translationally repressed. Kinases Gcn2, Vps34, and TOR act together to synergistically promote the ribosome or helicase recruitment on the 5′-mRNA cap. Studies are under way to understand the molecular mechanisms by which the Gcn2, TOR, and Vps34 pathways and their downstream targets contribute to *HAC1* mRNA translational derepression and promote ER stress response either directly or indirectly.

MATERIALS AND METHODS

Yeast strains, growth, gene disruption, and plasmids. Standard *S. cerevisiae* medium was used to grow and analyze the yeast strains. The genomic DNA of the *hac1::hphMX* strain was used as a template to amplify the *hphMX* cassette using primers annealing ~200 bases upstream and downstream of the *HAC1* open reading frame. The amplified PCR product was used to disrupt the *HAC1* gene of the *gcn2::kanMX* strain. Similarly, the genomic DNA of the *ire1::hphMX* strain was used as a template to amplify the *hphMX* cassette using primers annealing ~200 bases upstream and downstream of the *IRE1* open reading frame. The amplified PCR product was used to disrupt the *IRE1* gene in the *tor1*Δ *tor2*^{ts} strain and the *vps15::kanMX* strain. The list of yeast strains used in this study is shown in Table 1.

Plasmids were generated using the standard gene manipulation techniques. Mutation was generated by fusion PCR using standard protocols. The desired mutation in each plasmid was confirmed by Sanger sequencing. The list of plasmids used in this study are shown in Table 2.

Whole-cell extract preparation and Western blot analysis. Yeast cells were grown in yeast extract-peptone-dextrose (YEPD) or synthetic complete (SC) medium without appropriate nutrients until the optical density at 600 nm (OD_{600}) value reached ~0.6. Then, DTT (5 mM) or tunicamycin (0.5 μg/ml) was added to the medium to induce ER stress, and cells were harvested after 1 h (unless otherwise indicated). Whole-cell extracts (WCEs) were prepared by trichloroacetic acid (TCA) method as described previously (63). Proteins were fractioned by SDS-PAGE and subjected to Western blot analysis using rabbit anti-Hac1 (generated in our lab), mouse anti-PGK1 (catalog number 459250; Invitrogen), and rabbit anti-eIF2α (catalog number 9722; Cell Signaling, USA) antibodies. Each experiment was repeated at least twice, and a representative result is shown.

RNA analysis and RT-PCR. Yeast cells were grown in YEPD or SC medium without appropriate nutrients at 30°C to the OD_{600} value of ~0.5 to 0.6. DTT (5 mM) or tunicamycin (0.5 μg/ml) was added to the medium to induce the ER stress, and cells were grown further for another 1 h (unless otherwise indicated). Cells were harvested, and total RNA was isolated using the RNeasy minikit (Qiagen). Purified RNA was quantified using a Nanodrop spectrophotometer (ND-1000; Thermo Scientific) and treated with DNase I to remove genomic DNA contamination. One microgram of purified RNA was used to synthesize the first strand cDNA by a SuperScript III reverse transcriptase (Invitrogen; 18080-093) and a reverse primer (5′-CCCACCAACAGCGATAATAACGAG-3′) that corresponded to nucleotides +1002 to 1025. To assay *HAC1* mRNA expression, the synthetic cDNA was amplified by two exon 1-specific primers of *HAC1* mRNA

TABLE 2 List of plasmids used in this study

Plasmid name	Plasmid description	Reference or study
D3	pRS315, low-copy-no. *LEU2* vector	Lab collection
D4	pRS316, low-copy-no. *URA3* vector	Lab collection
D50	UPRE-LacZ in pRS425	This study
D72	IRE1 in D3	39
D2091	IRE1 in Yes2 vector	This study
D63	HAC1 in D4	9
D426	HAC1-C658G in D4	This study
D429	HAC1-G666C in D4	This study
D430	HAC1-C658G,G666C in D4	This study
D435	HAC1-U910G in D4	This study
D444	HAC1-G918U in D4	This study
D446	HAC1-U910G,G918U in D4	This study
D436	HAC1-U910C in D4	This study
D1694	HAC1-G771A in D4	9
D803	HAC1-G661C,G771A	9
D1025	HAC1-C-32A in D4	This study
D69	HAC1^{c} (intronless) in D4	This study
D2309	Tor2	67
D2310	Tor2-D2298E	67

(forward primer 5′-TCGCAATCGAACTTGGCTATCCCTACC-3′) and reverse primer 5′-CCAATTGTCAA GATCAATTGAATTGTC-3′). To assay *HAC1* mRNA splicing, the synthetic cDNA was then PCR amplified using a forward primer (5′-CGCAATCGAACTTGGCTATCCCTACC-3′) that corresponds to nucleotides +35 to 60 and a reverse primer (5′-CCCACCAACAGCGATAATAACGAG-3′) that corresponds to nucleotides +1002 to 1025. The PCR-amplified products were then run on a 1.5% agarose gel to separate spliced (HAC1^{s}) and unspliced (HAC1^{u}) forms of *HAC1* mRNA. Quantities of HAC1^{s} and HAC1^{u} were measured by ImageJ software. Percent splicing was calculated as Hac1^{s}/(HAC1^{s} + HAC1^{u}) · 100%. Each experiment was repeated at least two times.

***In vitro* reconstitution of the 5′-UTR and intron interaction.** Three target RNA oligonucleotides (20 nucleotides long) of 5′-UTR and intron were synthesized from Sigma (USA) as follows: (i) R1, representing the 5′-UTR (5′-UAACCUCCUCCUCCCCCACC-3′); (ii) R2, intron (5′-GAUGGGGGAGGAGCCGGUUG-3′); and (iii) R3, intron-G771A mutation (5′-GAUGGGGAAGGAGCCGGUUG-3′; underlining indicates that guanine was mutated to adenine). The RNA oligonucleotides R1 and R2 and R1 and R3 were mixed separately and heated to 95°C for 5 min and then annealed at room temperature slowly for an hour. The RNA mixture was diluted in 25 mM Tris-HCl, pH 8.0, to obtain final concentrations ranging from 50 nM to 1,000 nM. The SYBR green (100 μM; Life Technologies, USA) was diluted to 0.25 μM and added to each sample. The fluorescence intensity of 50 μl of each sample (three replicates) was then read in a BMG POLARStar plate reader using a Greiner black half-area 96-well plate (Ex, 497 nm; Em, 520 nm). The fluorescence intensities were plotted and analyzed by GraphPad Prism to estimate the equilibrium-binding affinity (K_d) values.

UPRE-driven LacZ reporter assay. Yeast cell was transformed with a *URA3* (D49) or *LEU2* (D50) plasmid containing a *LacZ* reporter gene under the control of a UPR element (UPRE) of the yeast *KAR2* gene (64). Yeast cells containing the UPRE-driven *LacZ* gene were grown overnight, diluted to a OD_{600} of ~0.2 in a synthetic complete (SC) medium without uracil and allowed to grow until the OD_{600} value reached ~0.6 to 0.8. The culture was then split into two flasks as follows: half of the culture was grown in the presence of 5 mM DTT, and the remainder was grown without DTT. Cells were harvested after 4 h, and protein extracts were prepared. The β-galactosidase assay was performed as described previously (65). The experiment was repeated at least thrice, and the LacZ units were plotted and represented in a histogram with standard errors.

ACKNOWLEDGMENTS

This work was supported by a grant to M.D. from the U.S. National Institutes of Health (1R01GM124183).

J.K.U., S.B., and MD designed and performed the experiments. J.K.U. and M.D. wrote the manuscript.

REFERENCES

1. Luo Y, Na Z, Slavoff SA. 2018. P-bodies: composition, properties, and functions. Biochemistry 57:2424–2431. https://doi.org/10.1021/acs.biochem.7b01162.
2. Standart N, Weil D. 2018. P-bodies: cytosolic droplets for coordinated mRNA storage. Trends Genet 34:612–626. https://doi.org/10.1016/j.tig.2018.05.005.

3. Baker KE, Coller J. 2006. The many routes to regulating mRNA translation. Genome Biol 7:332. https://doi.org/10.1186/gb-2006-7-12-332.
4. Nissan T, Parker R. 2008. Analyzing P-bodies in Saccharomyces cerevisiae. Methods Enzymol 448:507–520. https://doi.org/10.1016/S0076-6879(08)02625-6.
5. Aragon T, van Anken E, Pincus D, Serafimova IM, Korennykh AV, Rubio CA, Walter P. 2009. Messenger RNA targeting to endoplasmic reticulum stress signalling sites. Nature 457:736–740. https://doi.org/10.1038/nature07641.
6. Mori K, Kawahara T, Yoshida H, Yanagi H, Yura T. 1996. Signalling from endoplasmic reticulum to nucleus: transcription factor with a basic-leucine zipper motif is required for the unfolded protein-response pathway. Genes Cells 1:803–817. https://doi.org/10.1046/j.1365-2443.1996.d01-274.x.
7. Cox JS, Walter P. 1996. A novel mechanism for regulating activity of a transcription factor that controls the unfolded protein response. Cell 87:391–404. https://doi.org/10.1016/S0092-8674(00)81360-4.
8. Ruegsegger U, Leber JH, Walter P. 2001. Block of HAC1 mRNA translation by long-range base pairing is released by cytoplasmic splicing upon induction of the unfolded protein response. Cell 107:103–114. https://doi.org/10.1016/S0092-8674(01)00505-0.
9. Sathe L, Bolinger C, Mannan MA, Dever TE, Dey M. 2015. Evidence that base-pairing interaction between intron and mRNA leader sequences inhibits initiation of HAC1 mRNA translation in yeast. J Biol Chem 290:21821–21832. https://doi.org/10.1074/jbc.M115.649335.
10. Mori K. 2015. The unfolded protein response: the dawn of a new field. Proc Jpn Acad Ser B Phys Biol Sci 91:469–480. https://doi.org/10.2183/pjab.91.469.
11. Cox JS, Shamu CE, Walter P. 1993. Transcriptional induction of genes encoding endoplasmic reticulum resident proteins requires a transmembrane protein kinase. Cell 73:1197–1206. https://doi.org/10.1016/0092-8674(93)90648-A.
12. Mori K, Ma W, Gething MJ, Sambrook J. 1993. A transmembrane protein with a cdc2+/CDC28-related kinase activity is required for signaling from the ER to the nucleus. Cell 74:743–756. https://doi.org/10.1016/0092-8674(93)90521-Q.
13. Gonzalez TN, Sidrauski C, Dorfler S, Walter P. 1999. Mechanism of non-spliceosomal mRNA splicing in the unfolded protein response pathway. EMBO J 18:3119–3132. https://doi.org/10.1093/emboj/18.11.3119.
14. Sidrauski C, Cox JS, Walter P. 1996. tRNA ligase is required for regulated mRNA splicing in the unfolded protein response. Cell 87:405–413. https://doi.org/10.1016/S0092-8674(00)81361-6.
15. Mori K, Ogawa N, Kawahara T, Yanagi H, Yura T. 2000. mRNA splicing-mediated C-terminal replacement of transcription factor Hac1p is required for efficient activation of the unfolded protein response. Proc Natl Acad Sci U S A 97:4660–4665. https://doi.org/10.1073/pnas.050010197.
16. Di Santo R, Aboulhouda S, Weinberg DE. 2016. The fail-safe mechanism of post-transcriptional silencing of unspliced HAC1 mRNA. Elife 5:e20069. https://doi.org/10.7554/eLife.20069.
17. Hooks KB, Griffiths-Jones S. 2011. Conserved RNA structures in the non-canonical Hac1/Xbp1 intron. RNA Biol 8:552–556. https://doi.org/10.4161/rna.8.4.15396.
18. Kozak M. 2002. Pushing the limits of the scanning mechanism for initiation of translation. Gene 299:1–34. https://doi.org/10.1016/S0378-1119(02)01056-9.
19. Hinnebusch AG. 2011. Molecular mechanism of scanning and start codon selection in eukaryotes. Microbiol Mol Biol Rev 75:434–467. https://doi.org/10.1128/MMBR.00008-11.
20. Travers KJ, Patil CK, Wodicka L, Lockhart DJ, Weissman JS, Walter P. 2000. Functional and genomic analyses reveal an essential coordination between the unfolded protein response and ER-associated degradation. Cell 101:249–258. https://doi.org/10.1016/S0092-8674(00)80835-1.
21. Hinnebusch AG. 2005. Translational regulation of GCN4 and the general amino acid control of yeast. Annu Rev Microbiol 59:407–450. https://doi.org/10.1146/annurev.micro.59.031805.133833.
22. Rostislavleva K, Soler N, Ohashi Y, Zhang L, Pardon E, Burke JE, Masson GR, Johnson C, Steyaert J, Ktistakis NT, Williams RL. 2015. Structure and flexibility of the endosomal Vps34 complex reveals the basis of its function on membranes. Science 350:aac7365. https://doi.org/10.1126/science.aac7365.
23. Schu PV, Takegawa K, Fry MJ, Stack JH, Waterfield MD, Emr SD. 1993. Phosphatidylinositol 3-kinase encoded by yeast VPS34 gene essential for protein sorting. Science 260:88–91. https://doi.org/10.1126/science.8385367.
24. Backer JM. 2016. The intricate regulation and complex functions of the class III phosphoinositide 3-kinase Vps34. Biochem J 473:2251–2271. https://doi.org/10.1042/BCJ20160170.
25. Pakos-Zebrucka K, Koryga I, Mnich K, Ljujic M, Samali A, Gorman AM. 2016. The integrated stress response. EMBO Rep 17:1374–1395. https://doi.org/10.15252/embr.201642195.
26. Saxton RA, Sabatini DM. 2017. mTOR signaling in growth, metabolism, and disease. Cell 169:361–371. https://doi.org/10.1016/j.cell.2017.03.035.
27. Wek RC. 2018. Role of eIF2alpha kinases in translational control and adaptation to cellular stress. Cold Spring Harb Perspect Biol 10:a032870. https://doi.org/10.1101/cshperspect.a032870.
28. Vattem KM, Wek RC. 2004. Reinitiation involving upstream ORFs regulates ATF4 mRNA translation in mammalian cells. Proc Natl Acad Sci U S A 101:11269–11274. https://doi.org/10.1073/pnas.0400541101.
29. Patil CK, Li H, Walter P. 2004. Gcn4p and novel upstream activating sequences regulate targets of the unfolded protein response. PLoS Biol 2:E246. https://doi.org/10.1371/journal.pbio.0020246.
30. Cherkasova VA, Hinnebusch AG. 2003. Translational control by TOR and TAP42 through dephosphorylation of eIF2alpha kinase GCN2. Genes Dev 17:859–872. https://doi.org/10.1101/gad.1069003.
31. Magnuson B, Ekim B, Fingar DC. 2012. Regulation and function of ribosomal protein S6 kinase (S6K) within mTOR signalling networks. Biochem J 441:1–21. https://doi.org/10.1042/BJ20110892.
32. Hay N, Sonenberg N. 2004. Upstream and downstream of mTOR. Genes Dev 18:1926–1945. https://doi.org/10.1101/gad.1212704.
33. Urban J, Soulard A, Huber A, Lippman S, Mukhopadhyay D, Deloche O, Wanke V, Anrather D, Ammerer G, Riezman H, Broach JR, De Virgilio C, Hall MN, Loewith R. 2007. Sch9 is a major target of TORC1 in Saccharomyces cerevisiae. Mol Cell 26:663–674. https://doi.org/10.1016/j.molcel.2007.04.020.
34. Cosentino GP, Schmelzle T, Haghighat A, Helliwell SB, Hall MN, Sonenberg N. 2000. Eap1p, a novel eukaryotic translation initiation factor 4E-associated protein in Saccharomyces cerevisiae. Mol Cell Biol 20:4604–4613. https://doi.org/10.1128/mcb.20.13.4604-4613.2000.
35. Feoktistova K, Tuvshintogs E, Do A, Fraser CS. 2013. Human eIF4E promotes mRNA restructuring by stimulating eIF4A helicase activity. Proc Natl Acad Sci U S A 110:13339–13344. https://doi.org/10.1073/pnas.1303781110.
36. Jackson RJ, Hellen CU, Pestova TV. 2010. The mechanism of eukaryotic translation initiation and principles of its regulation. Nat Rev Mol Cell Biol 11:113–127. https://doi.org/10.1038/nrm2838.
37. Schmidt A, Kunz J, Hall MN. 1996. TOR2 is required for organization of the actin cytoskeleton in yeast. Proc Natl Acad Sci U S A 93:13780–13785. https://doi.org/10.1073/pnas.93.24.13780.
38. Yanagitani K, Imagawa Y, Iwawaki T, Hosoda A, Saito M, Kimata Y, Kohno K. 2009. Cotranslational targeting of XBP1 protein to the membrane promotes cytoplasmic splicing of its own mRNA. Mol Cell 34:191–200. https://doi.org/10.1016/j.molcel.2009.02.033.
39. Lee KP, Dey M, Neculai D, Cao C, Dever TE, Sicheri F. 2008. Structure of the dual enzyme Ire1 reveals the basis for catalysis and regulation in nonconventional RNA splicing. Cell 132:89–100. https://doi.org/10.1016/j.cell.2007.10.057.
40. Korennykh AV, Egea PF, Korostelev AA, Finer-Moore J, Zhang C, Shokat KM, Stroud RM, Walter P. 2009. The unfolded protein response signals through high-order assembly of Ire1. Nature 457:687–693. https://doi.org/10.1038/nature07661.
41. Cherry PD, Peach SE, Hesselberth JR. 2019. Multiple decay events target HAC1 mRNA during splicing to regulate the unfolded protein response. Elife 8:e42262. https://doi.org/10.7554/eLife.42262.
42. Peschek J, Walter P. 2019. tRNA ligase structure reveals kinetic competition between non-conventional mRNA splicing and mRNA decay. Elife 8:e44199. https://doi.org/10.7554/eLife.44199.
43. Korennykh AV, Korostelev AA, Egea PF, Finer-Moore J, Stroud RM, Zhang C, Shokat KM, Walter P. 2011. Structural and functional basis for RNA cleavage by Ire1. BMC Biol 9:47. https://doi.org/10.1186/1741-7007-9-47.
44. Mori T, Ogasawara C, Inada T, Englert M, Beier H, Takezawa M, Endo T, Yoshihisa T. 2010. Dual functions of yeast tRNA ligase in the unfolded protein response: unconventional cytoplasmic splicing of HAC1 pre-mRNA is not sufficient to release translational attenuation. Mol Biol Cell 21:3722–3734. https://doi.org/10.1091/mbc.E10-08-0693.
45. Pesole G, Mignone F, Gissi C, Grillo G, Licciulli F, Liuni S. 2001. Structural and functional features of eukaryotic mRNA untranslated regions. Gene 276:73–81. https://doi.org/10.1016/S0378-1119(01)00674-6.
46. Lin Z, Li WH. 2012. Evolution of 5' untranslated region length and gene expression reprogramming in yeasts. Mol Biol Evol 29:81–89. https://doi.org/10.1093/molbev/msr143.

47. Davuluri RV, Suzuki Y, Sugano S, Zhang MQ. 2000. CART classification of human 5' UTR sequences. Genome Res 10:1807–1816. https://doi.org/10.1101/gr.GR-1460R.
48. Reyes-Herrera PH, Ficarra E, Acquaviva A, Macii E. 2011. miREE: miRNA recognition elements ensemble. BMC Bioinformatics 12:454. https://doi.org/10.1186/1471-2105-12-454.
49. Reinhart BJ, Slack FJ, Basson M, Pasquinelli AE, Bettinger JC, Rougvie AE, Horvitz HR, Ruvkun G. 2000. The 21-nucleotide let-7 RNA regulates developmental timing in Caenorhabditis elegans. Nature 403:901–906. https://doi.org/10.1038/35002607.
50. Kozak M. 1987. An analysis of 5'-noncoding sequences from 699 vertebrate messenger RNAs. Nucleic Acids Res 15:8125–8148. https://doi.org/10.1093/nar/15.20.8125.
51. Muckenthaler M, Gray NK, Hentze MW. 1998. IRP-1 binding to ferritin mRNA prevents the recruitment of the small ribosomal subunit by the cap-binding complex eIF4F. Mol Cell 2:383–388. https://doi.org/10.1016/S1097-2765(00)80282-8.
52. Stoneley M, Willis AE. 2004. Cellular internal ribosome entry segments: structures, trans-acting factors and regulation of gene expression. Oncogene 23:3200–3207. https://doi.org/10.1038/sj.onc.1207551.
53. Lee AS, Kranzusch PJ, Doudna JA, Cate JH. 2016. eIF3d is an mRNA cap-binding protein that is required for specialized translation initiation. Nature 536:96–99. https://doi.org/10.1038/nature18954.
54. Soto-Rifo R, Rubilar PS, Ohlmann T. 2013. The DEAD-box helicase DDX3 substitutes for the cap-binding protein eIF4E to promote compartmentalized translation initiation of the HIV-1 genomic RNA. Nucleic Acids Res 41:6286–6299. https://doi.org/10.1093/nar/gkt306.
55. Guan BJ, van Hoef V, Jobava R, Elroy-Stein O, Valasek LS, Cargnello M, Gao XH, Krokowski D, Merrick WC, Kimball SR, Komar AA, Koromilas AE, Wynshaw-Boris A, Topisirovic I, Larsson O, Hatzoglou M. 2017. A unique ISR program determines cellular responses to chronic stress. Mol Cell 68:885–900. https://doi.org/10.1016/j.molcel.2017.11.007.
56. Pisarev AV, Kolupaeva VG, Yusupov MM, Hellen CU, Pestova TV. 2008. Ribosomal position and contacts of mRNA in eukaryotic translation initiation complexes. EMBO J 27:1609–1621. https://doi.org/10.1038/emboj.2008.90.
57. Kozak M. 1991. A short leader sequence impairs the fidelity of initiation by eukaryotic ribosomes. Gene Expr 1:111–115.
58. Pisarev AV, Kolupaeva VG, Pisareva VP, Merrick WC, Hellen CU, Pestova TV. 2006. Specific functional interactions of nucleotides at key $^{-}3$ and $^{+}4$ positions flanking the initiation codon with components of the mammalian 48S translation initiation complex. Genes Dev 20:624–636. https://doi.org/10.1101/gad.1397906.
59. Archer SK, Shirokikh NE, Beilharz TH, Preiss T. 2016. Dynamics of ribosome scanning and recycling revealed by translation complex profiling. Nature 535:570–574. https://doi.org/10.1038/nature18647.
60. Hamanaka RB, Bennett BS, Cullinan SB, Diehl JA. 2005. PERK and GCN2 contribute to eIF2α phosphorylation and cell cycle arrest after activation of the unfolded protein response pathway. Mol Biol Cell 16:5493–5501. https://doi.org/10.1091/mbc.e05-03-0268.
61. Cutler NS, Pan X, Heitman J, Cardenas ME. 2001. The TOR signal transduction cascade controls cellular differentiation in response to nutrients. Mol Biol Cell 12:4103–4113. https://doi.org/10.1091/mbc.12.12.4103.
62. Yang J, Roe SM, Prickett TD, Brautigan DL, Barford D. 2007. The structure of Tap42/α4 reveals a tetratricopeptide repeat-like fold and provides insights into PP2A regulation. Biochemistry 46:8807–8815. https://doi.org/10.1021/bi7007118.
63. Mannan MA, Shadrick WR, Biener G, Shin BS, Anshu A, Raicu V, Frick DN, Dey M. 2013. An ire1-phk1 chimera reveals a dispensable role of autokinase activity in endoplasmic reticulum stress response. J Mol Biol 425:2083–2099. https://doi.org/10.1016/j.jmb.2013.02.036.
64. Normington K, Kohno K, Kozutsumi Y, Gething MJ, Sambrook J. 1989. S. cerevisiae encodes an essential protein homologous in sequence and function to mammalian BiP. Cell 57:1223–1236. https://doi.org/10.1016/0092-8674(89)90059-7.
65. Anshu A, Mannan MA, Chakraborty A, Chakrabarti S, Dey M. 2015. A novel role for protein kinase Kin2 in regulating HAC1 mRNA translocation, splicing, and translation. Mol Cell Biol 35:199–210. https://doi.org/10.1128/MCB.00981-14.
66. Helliwell SB, Wagner P, Kunz J, Deuter-Reinhard M, Henriquez R, Hall MN. 1994. TOR1 and TOR2 are structurally and functionally similar but not identical phosphatidylinositol kinase homologues in yeast. Mol Biol Cell 5:105–118. https://doi.org/10.1091/mbc.5.1.105.
67. Jiang Y, Broach JR. 1999. Tor proteins and protein phosphatase 2A reciprocally regulate Tap42 in controlling cell growth in yeast. EMBO J 18:2782–2792. https://doi.org/10.1093/emboj/18.10.2782.